Experimental Evidence of *s*-Wave Superconductivity in Bulk CaC_6

G. Lamura,* M. Aurino, G. Cifariello, E. Di Gennaro, and A. Andreone

CNR-INFM Coherentia and Department of Physics, University of Naples ''Federico II,'' I-80125, Napoli, Italy

N. Emery, C. Hérold, J.-F. Marêché, and P. Lagrange

Laboratoire de Chimie du Solide Minéral-UMR 7555, Université Henri Poincaré Nancy I, B.P. 239, 54506 Vandœuvre-lès-Nancy Cedex, France

(Received 11 January 2006; published 16 March 2006)

The temperature dependence of the in-plane magnetic penetration depth, $\lambda_{ab}(T)$, has been measured in a *c*-axis oriented polycrystalline CaC_6 bulk sample using a high-resolution mutual inductance technique. A clear exponential behavior of $\lambda_{ab}(T)$ has been observed at low temperatures, strongly suggesting isotropic *s*-wave pairing. Data fit using the standard BCS theory yields $\lambda_{ab}(0) = (720 \pm 80)$ Å and $\Delta(0) = (1.79 \pm 0.08)$ meV. The ratio $2\Delta(0)/k_BT_c = (3.6 \pm 0.2)$ gives indication for a weakly coupled superconductor.

DOI: 10.1103/PhysRevLett.96.107008 PACS numbers: 74.25.Nf, 74.70.Ad, 81.05.Uw

The recent discovery of superconductivity at 6.5 and 11.5 K in the graphite intercalation compounds (GICs) YbC_6 [1] and CaC_6 [1,2], respectively, has renewed theoretical interest in the physical properties of this class of materials [3–5]. Graphite intercalated with alkali metals was known to undergo a normal-to-superconducting transition since 1965 [6], with T_c increasing with a larger alkali-metal concentration (highest T_c of 5 K for NaC_2 [7]). Superconductivity in GICs with rare-earth metals was first discovered with the synthesis of YbC_6. CaC_6 first showed traces of superconductivity in a reduced quality sample [1], and only recently has a clear transition been put in evidence in high quality bulk samples [2]. These results open new perspectives in the physics of graphite. Its low conductivity can be greatly enhanced by a large number of reagents, continuously changing from a semimetallic to a good metallic behavior. The discovery of superconductivity at easily reachable temperatures can be helpful in understanding the correlation between the charge transfer to the graphene layers and T_c. It has been also proposed [8] that a deeper comprehension of the pairing mechanism in GICs can shed light on the intrinsic or proximity-induced superconductivity reported in carbon nanotubes [9], which are at the core of nanotechnology research.

The atomic structure of first stage GICs with metals usually consists of a stacking of graphene sheets (*ab* plane) arranged in a hexagonal configuration, with the intercalated atom occupying interlayer sites above the centers of the hexagons. As shown by Emery *et al.* [10], CaC_6 is the only member of the MC_6 metal-graphite compounds exhibiting a rhombohedral symmetry.

One of the main open questions making GICs an interesting class of superconducting materials is related to the nature of the pairing mechanism, whether it is driven by an ordinary electron-phonon interaction [4,5] or due to electronic correlations [3]. The possibility of an unconventional, excitonic or plasmonic, origin of superconductivity in GICs has been invoked because of the nature of the energy bands in these compounds. The intercalant atoms act as donors, thus producing a charge transfer to the carbon layers. This results in partially filled, mostly 2D in character, graphite π bands. In addition, in all compounds exhibiting superconductivity, an interlayer 3D *s* band, well separated from the graphene sheets and formed by nearly free electrons propagating in the interstitial space, crosses the Fermi surface and hybridizes with the π bands. It is interesting to note that the stronger the hybridization is, the higher T_c is [3]. A sandwich structure consisting of alternate layers of metal and semiconductor has been suggested as a favorable environment for the excitonic mechanism, since the metal ''free'' electrons can tunnel into the gap region of the semiconductor and interact with the excitons [11]. Low-energy plasmons have been proposed as the dominant contribution to superconductivity in metal-intercalated halide nitrides [12]. The recent analysis by Calandra and Mauri [5] and Mazin and Molodtsov [13], however, points out that a simple electron-phonon interaction between the intercalant *s*-band electrons and Ca in-plane and C out-of-plane phonons in CaC_6 and Yb phonons in YbC_6 may be sufficient to explain superconductivity in these GICs.

All that said, it seems clear that the experimental challenge for understanding the origin of superconductivity in these compounds should focus on the mechanism determining the pairing and on the role played by the interlayer *s* band. A first step in answering these questions is to determine the symmetry of the superconducting gap function and the nature of the elementary excitations. The magnetic penetration depth λ is known to be a very sensitive probe of the low-lying quasiparticle energy, and it is capable to give information, which is significant on the $\lambda(0)$ scale rather than on the coherence length $\xi(0)$ scale, as it occurs in other spectroscopic tools. This corresponds to a probe of the true ''bulk'' properties of a homogeneous superconductor. To this aim, we have performed the first high-resolution measurement of the in-plane magnetic penetration depth $\lambda_{ab}(T)$ on a c-axis grown polycrystalline sample of CaC_6. We find clear evidence of an exponentially activated behavior of $\lambda_{ab}(T)$, consistent with an s-wave symmetry of the gap function. In particular, the gap deduced from the data fit is in full agreement with the BCS weak coupling value (3.52).

Bulk CaC_6 has been synthesized from highly oriented pyrolytic graphite [2,10]. The reaction is carried out for ten days between a pyrolytic graphite platelet and a molten lithium-calcium alloy at around 350 °C, under very pure argon atmosphere. The reactive alloy has to be very rich in lithium, with a composition between 75 and 80 at. % of Li. Despite such a low calcium concentration, no lithium is present in the final reaction product, and calcium alone is intercalated into graphite. For a more detailed description of the technique, see [10], and references therein. The resulting samples are platelike polycrystals with the c axes of all the crystallites forming the highly oriented graphite parallel to each other, whereas in the perpendicular plane the material is disordered, leading to an average of a and b directions, denoted as ab. The data presented here have been taken on a sample having a roughly rectangular shape of about $2.5 \times 2.5\ \mathrm{mm}^2$ and thickness of 0.1 mm. The as-grown samples are shiny and silver in color but tarnish quickly in air. To ensure that the analysis is performed on a clean and nonreacted surface, we have studied the same sample before and immediately after cleaving it. We have measured the in-plane magnetic penetration depth $\lambda_{ab}(T)$ in the range 1.8 K–T_c by using a single-coil mutual inductance technique described in detail elsewhere [14]. The typical frequency and magnitude of the inducing field B_{ac} perpendicular to the film surface are 2–4 MHz and <0.1 mT, respectively. Care has been taken to always operate in the linear response regime, monitored by varying the applied magnetic field. No significant edge effects are expected in samples equal or larger than 2 times the coil diameter d, as in the present case ($d = 0.8$ mm) [15].

In Fig. 1, we report the inductive characterization of the critical temperature by observing the behavior of the resonant frequency f_0 and the signal amplitude A_0 in the transition region [14]. The onset of superconductivity is at $T_c^{\mathrm{on}} = (11.46 \pm 0.05)$ K, with a transition width $\Delta T_c = (0.40 \pm 0.05)$ K. No difference has been found either in T_c^{on} or in ΔT_c before and after cleaving the sample. In Fig. 2(a), we show the change of the in-plane magnetic penetration depth in the overall temperature range for the sample under test before and after cleavage. A much larger variation is observed in the former case, in comparison with the freshly cleaved sample. At low temperatures [Fig. 2(b)], this feature is even more evident.

We first analyze the above results at low temperatures within the framework of a standard BCS s-wave model.

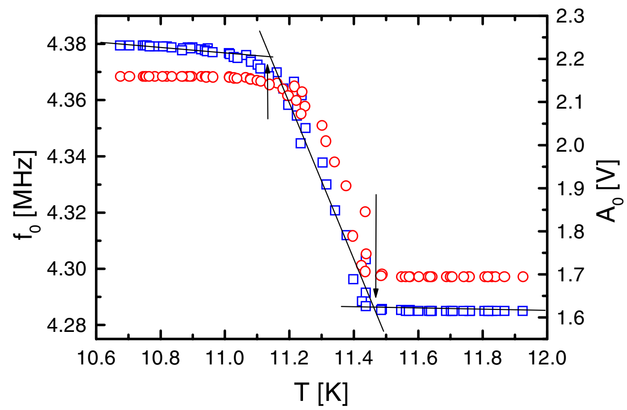

FIG. 1 (color online). T_c inductive characterization of CaC_6. At the superconducting transition, a large change in the resonant frequency f_0 (□) and amplitude A_0 (○) of the oscillating signal is observed. The arrows indicate the transition width ΔT_c. The solid lines are a guide for the eye.

According to the theory, the temperature dependence of $\Delta\lambda_{ab}$ is proportional to the fraction of normal electrons in the low-temperature limit ($T < T_c/2$) and follows a thermally activated behavior given by [16]:

$$\lambda(T) - \lambda(0) = \lambda(0)\sqrt{\frac{\pi\Delta(0)}{2k_B T}}\exp\left(-\frac{\Delta(0)}{k_B T}\right), \qquad (1)$$

where $\Delta(0)$ is the zero-temperature superconducting gap. In Fig. 2(b), we report also the result of a fit procedure performed by using Eq. (1) on the measurements carried out before and after cleavage (solid lines). In both cases, the BCS single-gap model well describes the data. In particular, for the freshly cleaved sample, the fit is extremely good, yielding the following superconducting parameters: $\Delta(0) = (1.79 \pm 0.08)$ meV and $\lambda_{ab}(0) = (720 \pm 80)$ Å. The ratio $2\Delta(0)/k_B T_c$ is then evaluated to be (3.6 ± 0.2). Before the cleavage, the same fit on the sample data gives a zero-temperature penetration depth almost doubled and a zero-temperature gap lowered by 30%. Such a difference in the behavior is very likely due to the presence of a thin [on the scale of $\lambda(0)$] reacted layer on the uncleaved sample surface, having depressed superconducting properties. This is confirmed by the fact that the inductively measured superconducting bulk transition is not affected by the degraded layer. For this reason, the discussion on the experimental data will focus only on the freshly cleaved sample. Using the results of the BCS fit at low temperatures, we then tried to deduce the London penetration depth in the ab plane over the whole temperature range from the relation [17]:

$$\lambda_L(T) = \lambda_{\mathrm{eff}}(T)\left[1 + \frac{\xi_{ab}(0)}{J(0,T)l_{\mathrm{mfp}}}\right]^{-1/2}, \qquad (2)$$

where $\xi_{ab}(0)$ is the zero-temperature in-plane coherence length, $l_{\mathrm{mfp}}(0)$ is the mean free path, and $J(0, T)$ is the real-

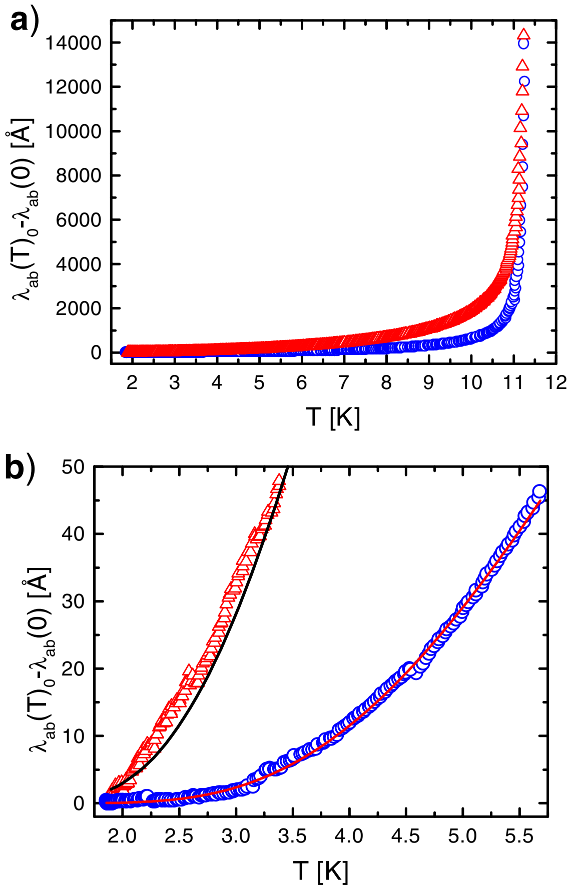

FIG. 2 (color online). (a) Variation of the in-plane magnetic penetration depth up to T_c for the sample under test before (△) and after cleavage (○). (b) The same as in (a) but at low temperatures ($T < T_c/2$). The solid lines represent the BCS fits (see text).

space kernel valid for a local electrodynamic response. The local limit can be safely used because $\xi_{ab}(0) = 350$ Å $< \lambda(0)$, by magnetization measurements performed in samples from the same batch [2]. The fit shows that the screening response of the CaC_6 sample is definitely in the dirty limit [$l_{\mathrm{mfp}}(0) < \xi_{ab}(0)$]. This can be also seen plotting the normalized superfluid density $n_s(T)/n_s(0) = [\lambda(0)/\lambda(T)]^2$ (Fig. 3). The experimental curve lies just between the clean local BCS limit and the two fluid behavior, and it is well described by the BCS calculation in the dirty limit [17] using the following equation:

$$\left[\frac{\lambda(0)}{\lambda(T)}\right]^2 = \frac{\Delta(T)}{\Delta(0)} \tanh\left(\frac{\Delta(T)}{2k_B T}\right). \tag{3}$$

This procedure allows us to confirm that the electrodynamic response of CaC_6 follows a single-gap s-wave behavior throughout the entire temperature range. However, nothing can be reliably said on the value of the mean free path and of the zero-temperature London penetration depth $\lambda_L(0)$. A precise estimation of $l_{\mathrm{mfp}}(0)$ confirming our conclusions must await an independent experiment. All that we can say is that, very likely, the dirty limit response is due to the presence of a certain amount of disorder in the Ca distribution during the intercalation process [18].

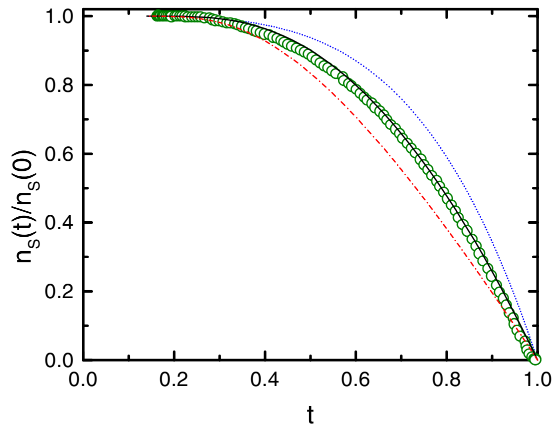

FIG. 3 (color online). Normalized superfluid density versus the reduced temperature for the cleaved sample (○). The short-dashed–dotted and the continuous lines represent the weakly coupled BCS model in the clean and in the dirty limit, respectively. The dotted line shows the two fluids behavior.

Since the variation of the magnetic penetration depth $\Delta\lambda(T)$ is proportional to the fraction of normal electrons in the low-temperature limit, it is useful to compare for CaC_6 this quantity versus the reduced temperature $t = T/T_c$ with data taken using the same technique on different superconductors: an optimally doped $YBa_2Cu_3O_{7-\delta}$ (Y123) single crystal [19], a $YBa_2Cu_4O_8$ (Y124) single crystal [20], and an epitaxial NbN thin film [21] (Fig. 4). In accordance with the d-wave model currently adopted for cuprates, $\Delta\lambda(T)$ follows a linear dependence for Y123 and Y124 samples. In the case of the s-wave BCS conventional superconductor NbN, the low-energy quasiparticle excita-

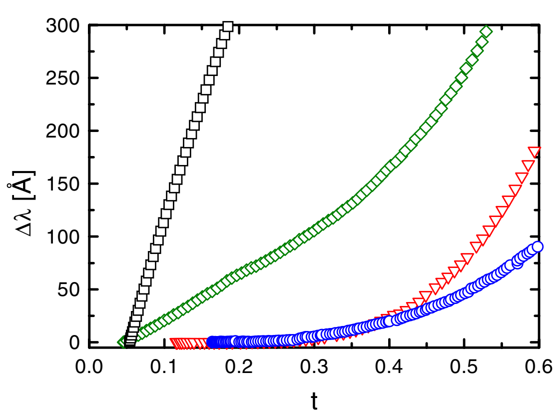

FIG. 4 (color online). Low-temperature variation of the in-plane magnetic penetration depth for different superconductors: a Y124 single crystal (□), a Y123 single crystal (◇), a NbN epitaxial thin film (▽), and the CaC_6 c-axis oriented polycrystalline sample under test (○).

tion rate is strongly reduced at low temperatures. The comparison shows that CaC_6 behaves as NbN does, providing further clear evidence of the fully gapped nature of superconductivity in this compound. Moreover, the measured ratio $2\Delta(0)/k_BT_c$ indicates that CaC_6 is a weakly coupled superconductor.

Finally, it is worth mentioning that GICs were believed to be an example of two-band gap superconductivity due to the crossing of the Fermi surface by both the graphite sheet π bands and the intercalant layer s band [22]. However, an attempt to fit the measurements using a two-band gap model [23] does not provide any additional information, simply because a single-gap analysis is fully capable to describe the data within a few percent indetermination. This result agrees with the prediction of Calandra and Mauri [5] that the contribution from the π bands is too small to sustain the superconductivity in CaC_6. Pairing is due mainly to the Ca s-band electrons coupled with C out-of plane and Ca in-plane phononic modes, thus giving origin to a single-gap s-wave superconductivity. In the framework of this model, by using the predicted values for the electron-phonon coupling $\lambda = 0.83$ and the logarithmic averaged phonon frequency $\omega_{ln} = 24.7$ meV [5], the expected ratio $2\Delta(0)/k_BT_c$ is 3.69 [24], which perfectly matches the measured value. Of course, the agreement does not rule out the possibility that the pairing mechanism be driven instead by electronic correlations.

In conclusion, we have reported the first measurement of the magnetic penetration depth in bulk CaC_6. A standard s-wave BCS model can account for the low-temperature experimental data, allowing a precise estimation of some superconducting parameters [$\Delta(0) = (1.79 \pm 0.08)$ meV and $\lambda_{ab}(0) = (720 \pm 80)$ Å]. The measured ratio $2\Delta(0)/k_BT_c = (3.6 \pm 0.2)$ points out that CaC_6 is a superconductor with weak coupling.

We thank A. Gauzzi for interesting and fruitful discussions. We are grateful to V. De Luise, A. Maggio, and S. Marrazzo for their valuable technical assistance.

*Author to whom correspondence should be addressed. Electronic address: gianrico.lamura@na.infn.it.

[1] T. E. Weller, M. Ellerby, A. S. Saxena, R. P. Smith, and N. T. Skipper, Nature Phys. **1**, 39 (2005).
[2] N. Emery, C. Hérold, M. d'Astuto, V. Garcia, C. Bellin, J. F. Marêché, P. Lagrange, and G. Loupias, Phys. Rev. Lett. **95**, 087003 (2005).
[3] G. Csányi, P. B. Littlewood, A. H. Nevidomskyy, C. P. Pikard, and B. D. Simons, Nature Phys. **1**, 42 (2005).
[4] I. I. Mazin, Phys. Rev. Lett. **95**, 227001 (2005).
[5] M. Calandra and F. Mauri, Phys. Rev. Lett. **95**, 237002 (2005).
[6] N. B. Hannay, T. H. Geballe, B. T. Matthias, K. Andres, P. Schmidt, and D. MacNair, Phys. Rev. Lett. **14**, 225 (1965).
[7] I. T. Belash, A. D. Bronnikov, O. V. Zharikov, and A. V. Palnichenko, Synth. Met. **36**, 283 (1990).
[8] T. M. Klapwijk, Nature Phys. **1**, 17 (2005).
[9] A. Kasumov, M. Kociak, M. Ferrier, R. Deblock, S. Guéron, B. Reulet, I. Khodos, O. Stéphan, and H. Bouchiat, Phys. Rev. B **68**, 214521 (2003).
[10] N. Emery, C. Hérold, and P. Lagrange, J. Solid State Chem. **178**, 2947 (2005).
[11] D. Allender, J. Bray, and J. Bardeen, Phys. Rev. B **7**, 1020 (1973).
[12] A. Bill, H. Morawitz, and V. Z. Kresin, Phys. Rev. B **68**, 144519 (2003).
[13] I. I. Mazin and S. L. Molodtsov, Phys. Rev. B **72**, 172504 (2005).
[14] A. Gauzzi, J. L. Cochec, G. Lamura, B. J. Jönsson, V. A. Gasparov, F. R. Ladan, B. Plaçais, P. A. Probst, D. Pavuna, and J. Bok, Rev. Sci. Instrum. **71**, 2147 (2000).
[15] G. Lamura, J. L. Cochec, A. Gauzzi, F. Licci, D. D. Castro, A. Bianconi, and J. Bok, Phys. Rev. B **67**, 144518 (2003).
[16] J. P. Turneaure, J. Halbritter, and H. A. Schwettman, J. Supercond. **4**, 341 (1991).
[17] M. Tinkham, *Introduction to Superconductivity* (McGraw-Hill, New York, 1996).
[18] M. S. Dresselhaus and G. Dresselhaus, Adv. Phys. **51**, 1 (2002).
[19] A. Erb, E. Walker, and R. Flükiger, Physica (Amsterdam) **245C**, 245 (1995).
[20] G. Lamura, A. Gauzzi, S. Kazakov, J. Karpinski, and A. Andreone, J. Phys. Chem. Solids (to be published).
[21] G. Lamura, J. C. Villégier, A. Gauzzi, J. L. Cochec, J.-Y. Laval, B. Plaçais, N. Hadacek, and J. Bok, Phys. Rev. B **65**, 104507 (2002).
[22] R. Al-Jishi, Phys. Rev. B **28**, 112 (1983).
[23] G. Lamura *et al.*, Phys. Rev. B **65**, 020506 (2002).
[24] F. Marsiglio, J. P. Carbotte, and J. Blezius, Phys. Rev. B **41**, 6457 (1990).